

The Effect of Coating Parameter on Properties of Plasma Sprayed Co Based Coatings

Serkan ÖZEL

Abstract: In this study, the surface of stainless steel was coated by Co based (Co, Mo, Cr) powders using plasma spray technique with different production parameters (500A, 550 A and 600 A current values) The coating layers were examined with optical microscopy, SEM, EDS and XRD analysis. The bonding strength of specimens was measured. In XRD studies, such compounds as $\text{Co}_3\text{Mo}_2\text{Si}$, CoMoSi , Co_2Mo_3 , Co_3Mo and Mo_5Si_3 have been identified on coating layers. The maximum hardness value has been determined in the specimen coated with 600 A.

Keywords: stainless steel; Co; plasma spray coating; microstructure; bonding strength

1 INTRODUCTION

Thermal barrier coatings (TBCs) are a method extensively utilized in a wide area of applications to protect surface against wear, corrosion and high temperature in industry such as gas turbines, aerial crafts, etc. [1-4]. One of the thermal spraying methods: plasma-spraying method offers very important gains such as wear resistance, temperature corrosion etc. in many materials including metals and their alloys, ceramics, cermets, some plastic which enables the coatings tools to be used for biomedical, electrical and thermal purposes [5]. In plasma sprayed coating powder particles are melted and deposited over the substrate by plasma jet. The temperature of plasma jet is over 7000 K to 20000 K, which melts any hard materials. Inside plasma jet usually blend of Ar is employed as a primary gas and H_2 as a secondary gas. An electric arc ionizes those gases. Therefore this method can be applied to manufacture materials, those that cannot be manufactured in any conventional way [6-9]. Based on the characteristics of the used powder and plasma spray gun APS coating has a considerable size of porosity which ranges from 1 to 40 vol % and coating can be deposited from 0,05mm to 0,5 mm [4, 10].

Austenitic stainless steel is one of the most important iron alloys used in structural applications due to its superior corrosion resistance, mechanical strength and ductility in oxidizing environments. Stainless steel with high chromium content is often used as engineering material. It is rarely used in tribological applications such as abrasion due to low surface hardness and load capacity [11].

Cobalt (Co) based alloys are widely used in orthopedic implants due to their high strength, good biocompatibility and wear resistance [12]. In the coating of Co-based alloys, besides the selection of special coating techniques, economical factors should be considered. Stainless steels coated with porous Co-Cr-Mo alloys are used as alternative materials because they are cheaper than Ti or Co-Cr-Mo

alloys. CoMoCrSi, rigid and low friction material, exhibits good sliding wear and oxidation resistance around the processing temperature of 800 °C. With these coatings, properties such as fatigue resistance, wear resistance and corrosion resistance of steel can be improved [13, 14]. Triballoy alloys are high wear and corrosion-resistant alloys which contain Ni or Co based materials. Therefore, they are preferable for excessive load and corrosive environments. The Laves phase is the reason for this alloy to have such characteristics. This phase governs all the material properties if the alloys are between 35-70 vol.% [15-17].

In the present study, Co based (Co, Mo, Cr) powders were coated on stainless steel using plasma spray technique with different production parameters. The influence of different production parameters in plasma spray technique applied to Co based coatings on the microstructure and surface roughness has been investigated.

2 EXPERIMENTAL PROCEDURE

2.1 Materials

The Co based (Co, Mo, Cr) powders were deposited on stainless steel substrate prepared in $80 \times 20 \times 10$ mm dimensions with a thickness between 200-320 μm , using a plasma spray technique. The Co based powder was provided from SulzerMetco. The Metco 66F-NS powder was used as a standard powder. Chemical composition by % weight of stainless steel substrate and Co based powder are given in Tab. 1. In order to produce a rough surface for good bonding, the stainless steel substrates were grid-blasted with alumina grits prior to the coating process.

Table 1 The chemical compositions of substrate material

Alloy	Weight (%) Composition					
	Fe	Cr	Ni	Mn	C	Si
Stainless Steel	Balance	18,26	8,24	1,76	0,06	0,35

Table 2 Properties of powder used in this study

Coating Powder	% Co	% Mo	% Cr	% Si	SulzerMetco Code	Particle Size (μm)
Co-Mo-Cr	Balance	28	8	2	66F-NS	-45 + 15

2.2 Plasma Spray Technique

Plasma spray coatings were produced by using manually 3 MB gun with this technique (Fig. 1). Plasma

spraying parameters used during the coating process are given in Tab. 2. The specimens are produced with different current in plasma spray technique.

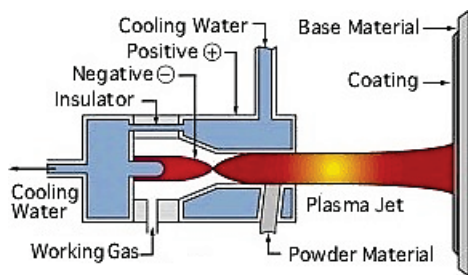


Figure 1 Schematic cross-section of a typical plasma spray

Table 3 Plasma spray coating parameters

Parameters	Specimens		
	S1	S2	S3
Current	500 A	550 A	600 A
Voltage	65 V	65 V	65 V
Gun Type	3 MB	3 MB	3 MB
Plasma Gas	125 l/dk Ar 15 l/dk H ₂	125 l/dk Ar 15 l/dk H ₂	125 l/dk Ar 15 l/dk H ₂
Spray Distance	100 mm	100 mm	100 mm

2.3 Microstructural Characterization and Mechanical Testings

400, 600, 800 and 1200 mesh SiC abrasive papers are used to grind the specimens, which are cut in cross-sectional layer and then polished with diamond paste. The etching process has not been applied to the sample after polishing. Microscopic structure is observed by optical microscope and SEM. EDS analyses for element analysis and X-ray diffraction (XRD) for compound analysis are performed. Qness-10M microhardness tester is used for microhardness measurements. The microhardness measurements were calculated with arithmetic mean of measured values from ten different regions for each sample. An epoxy adhesive is chosen to glue coating layer to pull road and 2h have been waited at 200 °C to dry. Adhesion test ASTM C-633 is applied to test the bonding strength of coating.

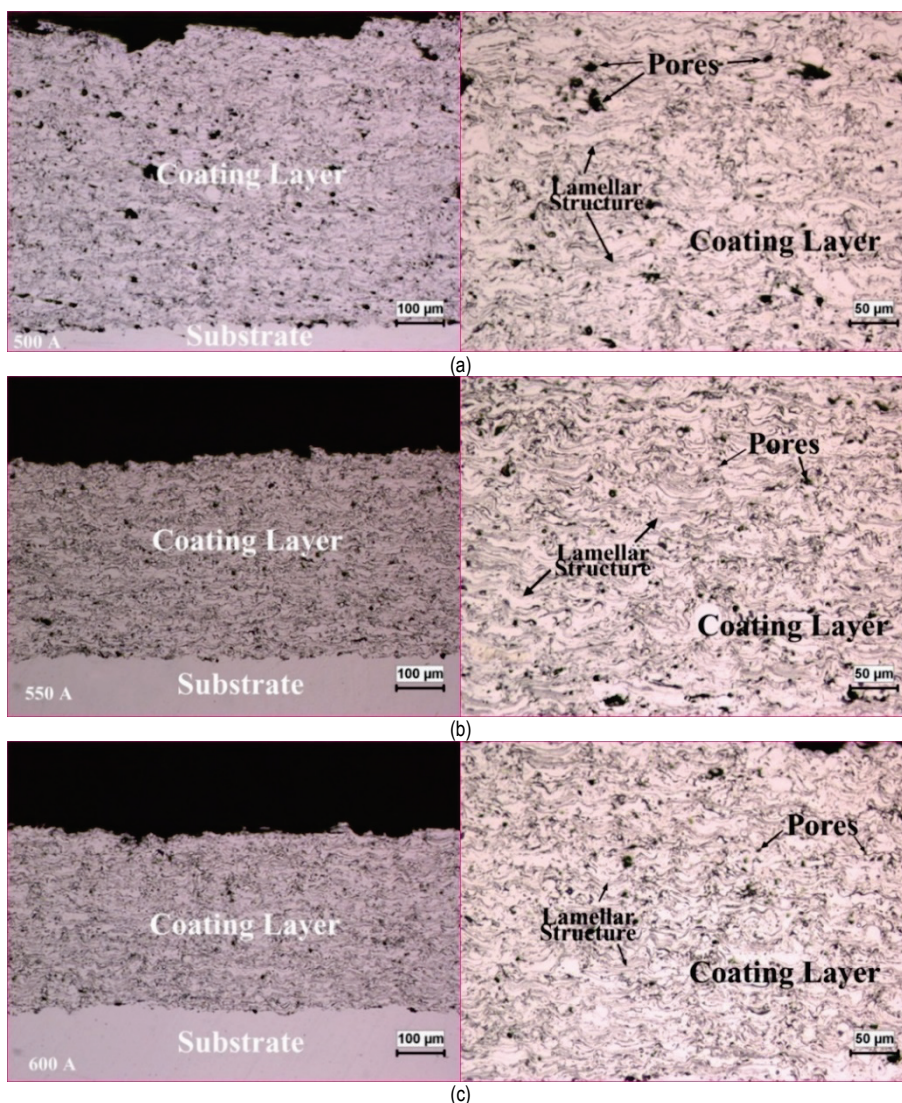


Figure 2 Microstructure pictures of specimens coated plasma spray technique, a) S1 specimen, b) S2 specimen and c) S3 specimen

3 RESULTS AND DISCUSSION

3.1 Microstructure Analysis of Coating Layer

Fig. 2 shows the optical microstructures of Co based coatings performed on the austenitic stainless steel surface by the plasma spray technique. The lamellar microstructure

is characteristic for thermal spray coating. The formation of the lamellar microstructure is shown at S1, S2 and S3 specimens, which are coated by plasma spray technique. On the stainless steel substrate 270-400 micron coating layers were achieved. After testing the specimens it is

shown that porous structures are formed in the coating layers. S1 specimen has a larger pore volume than the other specimens (Fig. 2a). The amount of pores decreased with the increase of current value applied during coating. The lowest pore volume was obtained in the coating layer of specimen S3 (Fig. 2c). In the plasma spraying method, increasing the plasma power causes the temperature of the

dust particles to increase. The hotter particles wet the surface better, resulting in a dense, less porous coating layer [18, 19]. Fig. 3a shows the SEM microstructure picture of coating layer at the S3 specimen and points taken by EDS analysis. The analysis of coating layer at the S3 specimen by EDS detected elements of Co, Mo, Cr and Si as shown in Fig. 3b, 3c, 3d, 3e.

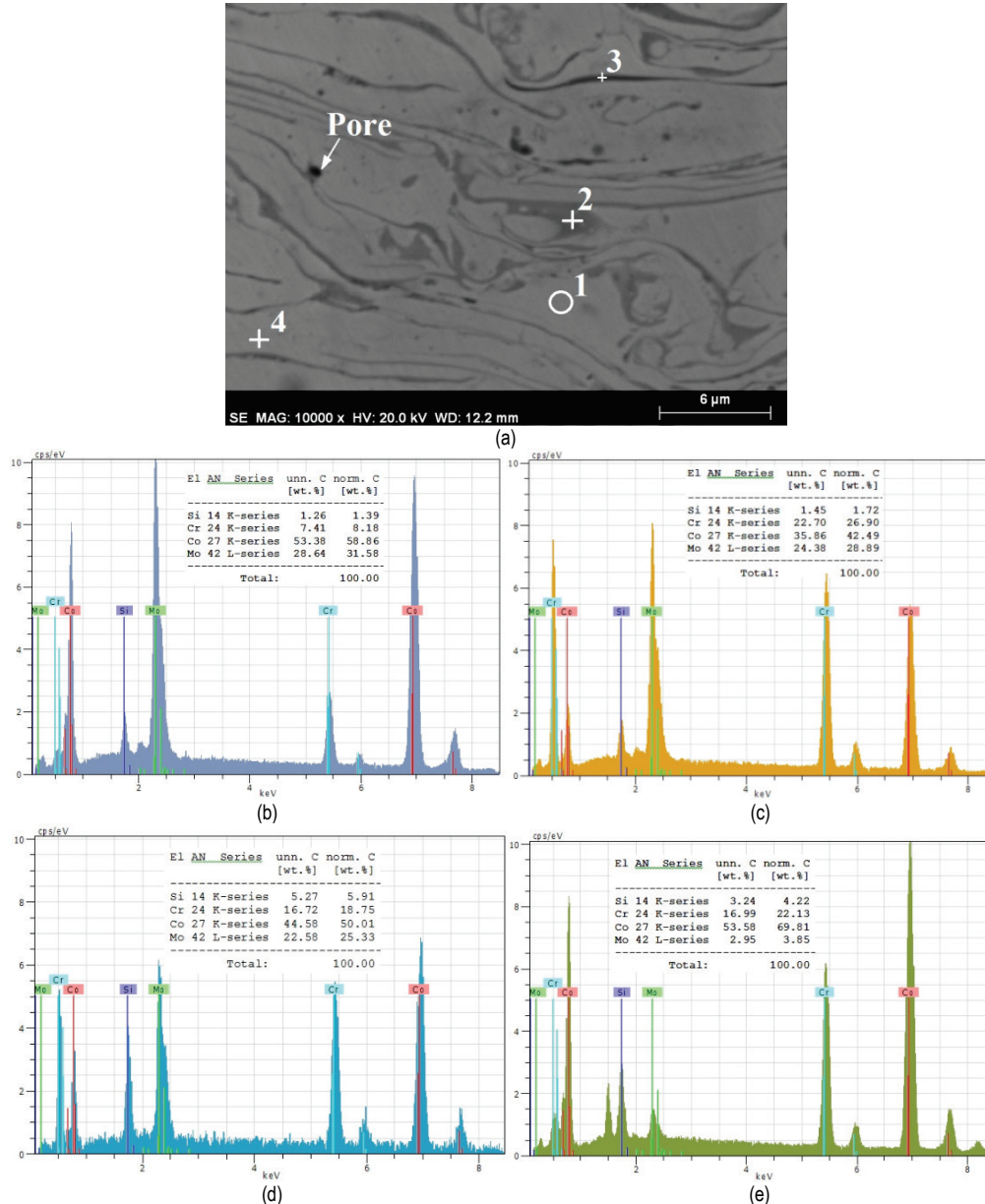


Figure 3(a) SEM microstructure picture of S3 specimen, (b) EDS analysis of the zone number 1, (c) EDS analysis of the point number 2, (d) EDS analysis of the point number 3, (e) EDS analysis of the point number 4.

The EDX analysis taken from gray and dark grey lamella region gave Co, Mo, Cr and Si elements for Point 2 and Point 3 (Fig. 3c, 3d). At Point 3, the Si ratio is the highest. The composition of the plotted light grey region at Point 4 in Fig. 3a consisted of 69.81 % Co, 22.13% Cr, 4.22% Si and 3.85 Mo. The highest value of the Co element was determined at Point 4. The EDS analysis results are in accordance with the compounds indicated in the XRD results.

The XRD patterns of Co-Mo-Cr powder coated specimens are shown in Fig. 4. In the specimens coated

with different current values, $\text{Co}_3\text{Mo}_2\text{Si}$, CoMoSi , Co_2Mo_3 , Co_3Mo compounds were formed in common. Laves phase (intermetallic phase) is formed in Co-Mo-Cr-Si alloy systems. The Laves phase consists of a hexagonal close packed (hcp). This phase is a composite of Co, Mo, and Si (like $\text{Co}_3\text{Mo}_2\text{Si}$ and/or CoMoSi). Since Laves phase's dislocation glide operation is complicated, these phases are strong and brittle. Laves phase has the Vickers hardness which is between 1000-1200. Generally its hardness depends on its composition and how it is produced [20, 21, 22].

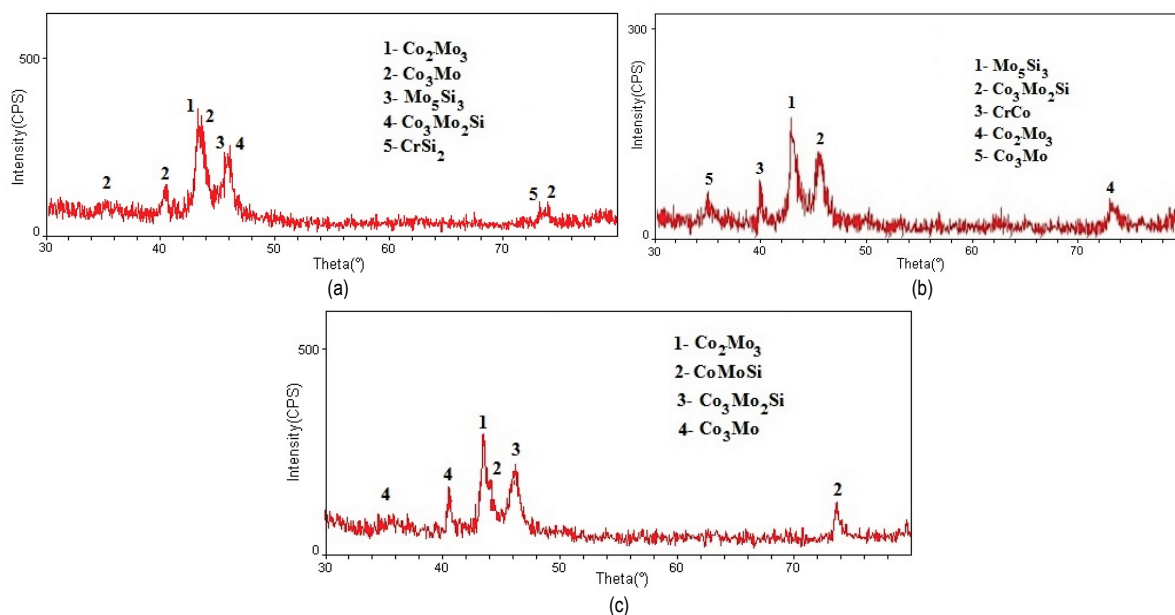


Figure 4 XRD analysis of specimens, (a) S1 specimen, (b) S2 specimen, (c) S3 specimen.

3.2 Microhardness Tests

The microhardness measurement results taken from the coating layers are shown in Fig. 5. The microhardness values of coating layers of S1, S2 and S3 specimens are 415, 462 and 570 HV, respectively. Maximum microhardness was measured in the S3 specimen coated with 600 A current value. Fig. 2 shows that the porosity was decreased with increase of current value. In the plasma spraying method, the plasma power was increased by increasing the current value. With the increase of the plasma power, a less porous coating layer was obtained [18, 19]. Microhardness value decreases with increased porosity value [23]. Minimum microhardness value was measured in the S1 specimen coated with 500 A current value.

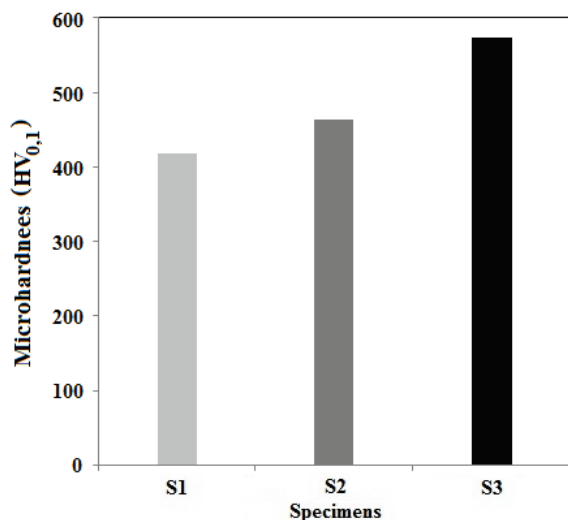


Figure 5 Microhardness values of coating layer of specimens

3.3 Bonding Strength Tests

The bonding strength of specimens coated with Co-Mo-Cr powder is shown in Fig. 6. Bonding strengths of coatings were tested using tensile test machine according

to ASTM C 633. The bonding strengths of S1, S2 and S3 coatings were 34.45 MPa, 42.46 MPa and 58.34 MPa, respectively. Maximum bonding strength was measured in the S3 specimen coated at 600 A current value. The adhesion strength between the substrate and the coating layer could be improved by decrease of porosity at S3 specimen.

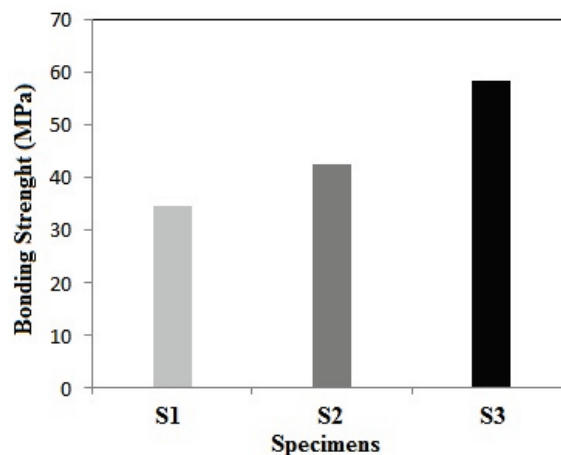


Figure 6 Bonding Strengths of coating layer of specimens

4 CONCLUSIONS

In this study, plasma sprayed Co based coatings on stainless steel alloy were fabricated, and their microstructure, hardness and bonding strength were investigated using optical microscope, SEM, EDX, XRD, microhardness and bonding strength test.

- 1) Typical lamellar structures existed in Co based coatings. The porosity exists in all coatings. The pore amount was decreased with increasing of current value at plasma spray process.
- 2) Similar phases are $\text{Co}_3\text{Mo}_2\text{Si}$, CoMoSi , Co_2Mo_3 , Co_3Mo in coating layer of S1, S2 and S3 specimens. However, Mo_5Si_3 , CrSi_2 and CrCo phases were formed in coating layers.
- 3) Microhardness was increased with increase of current value. Maximum microhardness was measured in the

- S3 specimen coated with 600 A current value. Minimum microhardness value was measured in the S1 specimen coated with 500 A current value.
- 4) Maximum bonding strength was measured in the S3 specimen coated at 600 A current value. The adhesion strength between the substrate and the coating layer could be improved by decrease of porosity at S3 specimen.

Acknowledgement

The author would like to thanks the Bitlis Eren University Science and Technology Research and Application Center for tests of specimens and Turkish Airlines Technic Inc. for the coatings and bonding strength tests.

5 REFERENCES

- [1] Ma, R., Cheng, X., & Ye, W. (2015). SiC fiber and yttria-stabilized zirconia composite thick thermal barrier coatings fabricated by plasma spray. *Applied Surface Science*, 357, 407-412. <https://doi.org/10.1016/j.apsusc.2015.09.028>
- [2] Mishra, S. B., Chandra, K., & Prakash, S. (2017). Studies on erosion-corrosion behaviour of plasma sprayed Ni3Al coating in a coal-fired thermal power plant environment at 540 °C. *Anti-Corrosion Methods and Materials*, 64(5), 540-549. <https://doi.org/10.1108/ACMM-11-2015-1592>
- [3] Wood, R. J. K. (2010). Tribology of thermal sprayed WC-Coatings. *International Journal of Refractory Metals and Hard Materials*, 28(1), 82-94. <https://doi.org/10.1016/j.ijrmhm.2009.07.011>
- [4] Nor, A. M., Abbas, M. R., Rajoo, S., Md Sah, M. H., & Ahmad, N. (2014). Review on Ceramic Application in Automotive Turbo charged Engines. *Applied Mechanics and Materials*, 660, 219-228. <https://doi.org/10.4028/www.scientific.net/AMM.660.219>
- [5] Özel, S. & Turhan, H. (2010). The Microstructure and hardness properties of ZrO₂+Y₂O₃/Al₂O₃ layers coated by using plasma spray process on Al bronze surface, *Praktische Metallographie*, 10, 560-570. <https://doi.org/10.3139/147.110118>
- [6] Fauchais, P. L., Heberlein, J. V. R., & Boulos, M. I. (2014). *Thermal Spray Fundamentals: From Powder to Part*, London, Springer US Books. <https://doi.org/10.1007/978-0-387-68991-3>
- [7] Djebali, R., Pateyron, B., & El Ganaoui, M. (2015). Scrutiny of plasma spraying complexities with case study on the optimized conditions toward coating process control. *Case Studies in Thermal Engineering*, 6, 171-181. <https://doi.org/10.1016/j.csite.2015.09.005>
- [8] Özel, S. (2009). The investigation of coating of oxide and carbide compounds on the surface of aluminium alloy and bronze by using plasma spray process. *PhD Thesis*, Firat University, Turkey.
- [9] Bolelli, G., Cannillo, V., Lusvardi, L., & Manfredini, T. (2006). Glass-alumina composite coatings by plasma spraying. Part I: Microstructural and mechanical characterization. *Surface & Coating Technology*, 201(1-2), 458-473. <https://doi.org/10.1016/j.surfcoat.2005.10.039>
- [10] Tucker, R. C. (1994). *Thermal Spray Coatings-Surface Engineering*, Ohio, ASM Handbook.
- [11] Özel, S., Dikici, B., Somunkiran, İ., & Gavgalı, M. (2008). The Corrosion Characteristic of Alloyed NiTi Powder Mixture on Austenitic Stainless Steel by Using PTA Process, *XI. International Corrosion Symposium, Izmir, Turkey*, 665-671.
- [12] Sarıkaya, M. & Güllü, A. (2015). Multi-response optimization of minimum quantity lubrication parameters using Taguchi-based grey relational analysis in turning of difficult-to-cut alloy Haynes 25. *Journal of Cleaner Production*, 91, 347-357. <https://doi.org/10.1016/j.jclepro.2014.12.020>
- [13] Ozols, A., Barreiro, M., Forlerer, E., & Sirkin, H. R. (2006). Coating of Co-Cr-Mo alloy for surgical implants by centrifugal spray: Preliminary evaluation. *Surface & Coating Technology*, 200, 5884-5888. <https://doi.org/10.1016/j.surfcoat.2005.08.139>
- [14] Fauchais P. and Vardelle, A. (2012). *Thermal Sprayed Coatings Used Against Corrosion and Corrosive Wear, Advanced Plasma Spray Applications*, InTech, France. Retrieved from <http://www.intechopen.com/books/advanced-plasma-spray-applications/thermal-sprayed-coatings-used-against-corrosion-and-corrosive-wear>
- [15] Gao, F., Liu, R., & Wu, X. J. (2011). Triballoy alloy reinforced tin-bronze composite coating for journal bearing applications. *Thin Solid Films* 519, 4809-4817. <https://doi.org/10.1016/j.tsf.2011.01.035>
- [16] Zhang, S. & Zhao, D. (2012). *Advances in Materials Science and Engineering, Aerospace Materials Handbook*. CRC Press, London.
- [17] Jiang, K. (2013). Effects of Heat Treatment on Microstructure and Wear Resistance of Stainless Steels and Superalloys, *Master Thesis*, University of Ottawa, Canada. <https://doi.org/10.20381/ruor-3043>
- [18] Bengi, T. (2009). The Investigation of Thermal Properties of Thermal Barrier Coating and Parameter Optimization for Low Thermal Conductivity, *Master Thesis*, İstanbul Technical University, Turkey.
- [19] Scrivani, A., Rizzi, G., & Berndt, C. C. (2008). Enhanced thick thermal barrier coatings that exhibit varying porosity. *Materials Science and Engineering A*, 476, 1-7. <https://doi.org/10.1016/j.msea.2007.04.035>
- [20] Yao, M. X., Wu, J. B. C., Yick, S., Xie, Y., & Liu, R. (2006). High temperature wear and corrosion resistance of a Laves phase strengthened Co-Mo-Cr-Si alloy. *Materials Science and Engineering A*, 435-436, 78-83. <https://doi.org/10.1016/j.msea.2006.07.054>
- [21] Podrez-Radziszewska, M., Haimann, K., Dudziński, W., & Morawska-Soltysik, W. (2010). Characteristic of intermetallic phases in cast dental CoCrMo alloy, *Archives of Foundry Engineering*, 10(3), 51-56. Retrieved from <http://www.afe.polsl.pl/index.php/en/307/characteristic-of-intermetallic-phases-in-cast-dental-coormo-alloy.pdf>
- [22] Liu, R., Yao, J. H., Zhang, Q. L., Yao, M. X., & Collier, R. (2016). Effects of silicon content on the microstructure and mechanical properties of cobalt-based Triballoy alloys. *Journal of Engineering Materials and Technology*, 138(4), 1-7. Retrieved from <http://materialstechnology.asmedigitalcollection.asme.org/article.aspx?articleid=2533289&journalid=121>
- [23] Özel, S. & Turhan, H. (2011). The Effect of Cr₃C₂ on Microstructure and Hardness of Cu5Al Plasma Sprayed Coatings. *Praktische Metallographie*, 6, 321-330. <https://doi.org/10.3139/147.110118>

Contact information:

Serkan ÖZEL, Assoc. Prof. Dr.
Bitlis Eren University,
Faculty of Engineering Architectural,
Department of Mechanical Engineering,
13000 Bitlis / Turkey
sozel@beu.edu.tr